OFDM and analog RS/BCH codes

Werner Henkel and Fangning Hu
International University Bremen
{w.henkel, f.hu}@iu-bremen.de

***Abstract*— We discuss the relations between OFDM and Reed-Solomon codes, pointing out that OFDM can be seen as an analog RS code as soon as a cyclically consecutive range of carriers is not used for transmission, *i.e.*, carries zeros. Thus, these RS codes could be used for correction purposes before a standard channel decoder is invoked. We will concentrate on means of erasure decoding and point out useful applications, especially impulse-noise and clipping correction.**

***Index Terms*— OFDM, DMT, RS codes, BCH codes, analog codes**

I. Introduction

Analog RS and BCH codes are equivalent to OFDM and DMT, respectively, where a cyclically consecutive range of carriers is not used for transmission, *i.e.*, with zeros on it or reserved predefined signals (*e.g.* pilots). In this extended abstract, we give an overview over possible distortions where analog RS/BCH codes can be useful. We see three possible applications:

1) Correction of impulse noise
2) Clipping correction
3) Correction of frequency-selective fading

In here, we are focusing on the first two applications. One may realize that all applications are of bursty nature. A correction in an additive white noise environment is indeed not too useful, since then, no statistical bindings can be used to profit from for error correction. In this case, the best solution would just be to set the redundant positions to zero.

Notation: two underlines denote a matrix, one underline denotes a vector, $\underline{\underline{A}}_{i,j}$ denotes the (i,j)th entry of a matrix $\underline{\underline{A}}$, $\underline{\underline{A}}^{\theta_0,\ldots,\theta_t}_{\delta_0,\ldots,\delta_r}$ denotes rows $\theta_0,\ldots,\theta_t$ and columns $\delta_0,\ldots,\delta_r$ of a matrix $\underline{\underline{A}}$. Capital letters denote frequency-domain symbols, lowercase letters denote time-domain symbols.

This work is part of the FP6 / IST project M-Pipe and is co-funded by the European Commission.

II. Correction of impulse noise

This is the original application of analog codes. We use the correction capabilities according to the minimum Hamming distance of the code.

Non-stationary impulse noise can typically be found in wireline transmission (*e.g.* xDSL). In case of the twisted pairs of the telephone network, in former times, it was especially due to relay reopenings of mechanical switches in the central office. Furthermore, it results from fluorescent tubes, electrical engines, ignition, lighting, etc.. These sources of impulse noise are also valid for other media, like coaxial cables and power lines. Impulse noise disturbing only a few samples in time domain could effectively be corrected by an analog RS code[1]. Longer impulses are typically spectrally concentrated. The corresponding samples in DFT domain should at least be marked as erased to improve later error correction stages. Generally, erasure decoding will be chosen as non-iterative decoding procedure for the analog codes. Note that every erasure requires a single redundant sample. Determining the error positions by applying, *e.g.*, Berlekamp's algorithm would, of course, be possible, as well. However, our focus will be on low-complex solutions.

The major task will be to detect the impulses to mark the corresponding samples as erased or even to detect the spectral distribution to erase samples for later processing.

Additional to impulse noise there will at least be a dispersive channel. Equalization can be carried out after the whole decoding or before the IFFT at the transmitter (precoding). Filter responses before the impulse-noise correction will distribute the impulses thereby possibly exceeding the correction capability of the analog code. Thus, we may have the following two options for a procession chain.

$$\text{[S/P]} \longrightarrow \text{[QAM-Mapping]} \longrightarrow \text{[IFFT]} \longrightarrow \text{[CP Extension]} \longrightarrow \text{[Channel]} \longrightarrow$$

[1] In here, we only present results for DMT transmission, *i.e.*, analog BCH codes. However, since RS codes are more general, we may just speak of RS codes.

[CP Deletion] ⟶ [Erasure Marking] ⟶ [FFT] ⟶ [Analog Decoding] ⟶ [FEQ] ⟶ [P/S]

[S/P] ⟶ [QAM-Mapping] ⟶ [Precoding] ⟶ [IFFT] ⟶ [CP Extension] ⟶ [Channel] ⟶ [CP Deletion] ⟶ [Erasure Marking] ⟶ [FFT] ⟶ [Analog Decoding] ⟶ [P/S]

S/P stands for serial/parallel conversion, CP is the cyclic prefix (guard interval), FEQ is frequency-domain equalization.

A. Correction of impulse noise by shift register syndrome extension

The analog decoding can take place in the time and DFT domain. However, since the data is located in DFT domain one may, at first sight, prefer DFT-domain extension of the syndrome provided by a shift register circuit (see Fig. 1) derived from the well-known key equation of RS codes.

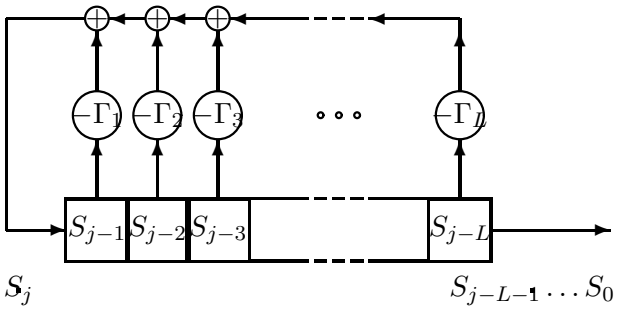

Fig. 1. Shift-register representation of the key equation

After extending the syndrome from the known parity positions to the whole codeword in DFT domain, it would be subtracted from the received word. However, one may realize that such a shift register solution would actually accumulate noise so that one may instead go for a least-squares procedure which is described in the following section.

B. Correction of impulse noise by least-squares decoding

Figure 2 shows the block diagram of impulse-noise correction in time domain by a least-squares approach. The received time domain vector $\underline{r}$ is written as

$$\underline{r} = \underline{x} + \underline{w} + \underline{\gamma} \,,$$

where $\underline{x}$ is the information vector in time domain, $\underline{w}$ is a vector of Gaussian noise samples, and $\underline{\gamma}$ is the impulse-noise vector.

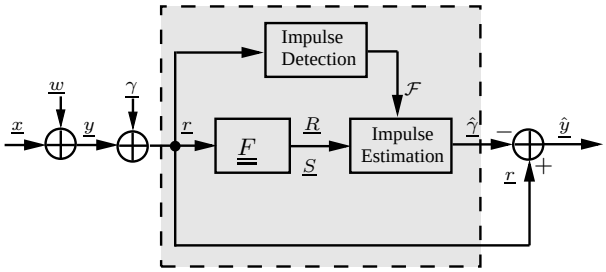

Fig. 2. Block diagram of the impulse-noise mitigation

Impulse noise is detected and declared as an erasure if the amplitude of the received symbol exceeds a certain threshold δ. In the next section, we will give a theoretical derivation of an optimal threshold to minimize the probability of false detection.

Let $\mathcal{F}$ be a set of indices of detected error locations defined as:

$$\mathcal{F} = \{f_i | \, |r_{f_i}| > \delta, i = 0, \ldots, e\} \,,$$

where f_i is the impulse location and e is the number of impulsive samples.

By performing a DFT of the received time domain vector $\underline{r}$, we obtain

$$\underline{R} = \underline{\underline{F}}\,\underline{r} = \underline{X} + \underline{\underline{F}}\,\underline{w} + \underline{\underline{F}}\,\underline{\gamma} \,, \tag{1}$$

where $\underline{X}$ is the information vector in the frequency domain. Let $\mathcal{L} = \{l_0, l_1, \ldots, l_m\}$ be the locations of the guard carriers, *i.e.*, the corresponding components ('rows') of $\underline{X}$ are zeros, $[\underline{X}]^{\mathcal{L}} = \underline{0}$. Then the corresponding components ('rows') of $\underline{R}$ only contains the frequency contents of impulse noise and Gaussian noise, *i.e.*,

$$[\underline{R}]^{\mathcal{L}} = [\underline{\underline{F}}]^{\mathcal{L}}\underline{w} + [\underline{\underline{F}}]^{\mathcal{L}}\underline{\gamma} \,. \tag{2}$$

In coding, $[\underline{R}]^{\mathcal{L}}$ is called the syndrome usually denoted by $\underline{S}$.
Notice that only e entries of $\underline{\gamma}$ with indices in $\mathcal{F}$ are non-zeros; Eqn. (2) can be rewritten as:

$$[\underline{R}]^{\mathcal{L}} = [\underline{\underline{F}}]^{\mathcal{L}}\underline{w} + [\underline{\underline{F}}]^{\mathcal{L}}_{\mathcal{F}}[\underline{\gamma}]^{\mathcal{F}} \,. \tag{3}$$

For simplicity, let $\underline{\underline{V}} = [\underline{\underline{F}}]^{\mathcal{L}}_{\mathcal{F}}$, $\underline{\underline{W}} = [\underline{\underline{F}}]^{\mathcal{L}}$. Then, Eqn. (3) reads

$$\underline{S} = \underline{\underline{V}}[\underline{\gamma}]^{\mathcal{F}} + \underline{\underline{W}}\underline{w}. \tag{4}$$

An estimate of $[\underline{\gamma}]^{\mathcal{F}}$ can be obtained by solving the above system of linear equations in the least-squares sense, resulting in [1]

$$[\hat{\underline{\gamma}}]^{\mathcal{F}} = (\underline{\underline{V}}^H\underline{\underline{V}})^{-1}\underline{\underline{V}}^H\underline{S} \,. \tag{5}$$

C. Optimal Threshold

Let H_0 and H_1 be the hypotheses for a sample r_k to contain or not to contain a noise impulse γ_k, respectively. As a simplification, we also assume the impulse noise to be Gaussian, *i.e.*, $\gamma_k \sim G(0, \sigma_\gamma)$, although we are aware that this is not exactly true in practice.

$$\begin{aligned} H_0: &\quad r_k = y_k = x_k + w_k \\ H_1: &\quad r_k = s_k = x_k + w_k + \gamma_k \end{aligned} \tag{6}$$

Since $y_k = x_k + w_k$ is the sum of two Gaussian random variables, $y_k \sim G(0, \sigma_{y_k}^2)$ is also a Gaussian with

$$\sigma_{y_k}^2 = \sigma_{x_k}^2 + \sigma_w^2 \; . \tag{7}$$

The one-sided density of the amplitude is two times the original Gaussian density.

$$p_{y_k}(|y_k|) = \frac{2}{\sqrt{2\pi}\sigma_{y_k}} e^{-\frac{|y_k|^2}{2\sigma_{y_k}^2}} \; . \tag{8}$$

This also holds for the amplitude of s_k with $\sigma_{s_k}^2 = \sigma_{y_k}^2 + \sigma_\gamma^2$

$$p_{s_k}(|s_k|) = \frac{2}{\sqrt{2\pi}\sigma_{s_k}} e^{-\frac{|s_k|^2}{2\sigma_{s_k}^2}} \; . \tag{9}$$

The conditional probabilities are

$$\begin{aligned} p(|r_k||H_0) &= p_{|y_k|}(|y_k| = |r_k|) = \frac{2}{\sqrt{2\pi}\sigma_{y_k}} e^{-\frac{|r_k|^2}{2\sigma_{y_k}^2}}, \\ p(|r_k||H_1) &= p_{|s_k|}(|s_k| = |r_k|) = \frac{2}{\sqrt{2\pi}\sigma_{s_k}} e^{-\frac{|r_k|^2}{2\sigma_{s_k}^2}} . \end{aligned} \tag{10}$$

Assume the probability of occurrence of an impulse noise is p, which means the *a priori* probabilities of occurrence of H_0, H_1 are $p(H_0) = 1 - p, p(H_1) = p$. We can compute the *a posteriori* ratio for each r_k as

$$\Lambda(r_k) = \frac{p(H_1|r_k)}{p(H_0|r_k)} = \frac{p(r_k|H_1)p(H_1)}{p(r_k|H_0)p(H_0)} \; . \tag{11}$$

According to Bayes, the decision criterion which minimizes the false detection probability is

$$\begin{aligned} H_0, &\quad \text{if} \quad \Lambda(r_k) < 1 \\ H_1, &\quad \text{if} \quad \Lambda(r_k) >= 1 \end{aligned} \tag{12}$$

Since $\Lambda(r_k)$ is monotonously increasing, an optimal decision threshold δ_k for r_k can be obtained by solving the equation $\Lambda(r_k = \delta_k) = 1$ which means $p(H_1|r_k = \delta_k) = p(H_0|r_k = \delta_k)$. Finally, the optimal threshold δ_k is computed as

$$\delta_k = \sqrt{\frac{2\sigma_{y_k}^2 \sigma_{s_k}^2 (\log \frac{\sigma_{s_k}}{\sigma_{y_k}} + \log \frac{1-p}{p})}{(\sigma_{s_k}^2 - \sigma_{y_k}^2)}} \; . \tag{13}$$

Figure 3 gives an example of the theoretical and simulated pdfs of $p(H_0|r_k)$ and $p(H_1|r_k)$ with $p = 0.5$, $\sigma_\gamma = 10V_{RMS}$ and $SNR = 16\,\text{dB}$ for a QPSK constellation. It is shown that the simulated results matches the theoretical curve. The optimal threshold δ_k is the point of intersection of the two pdfs.

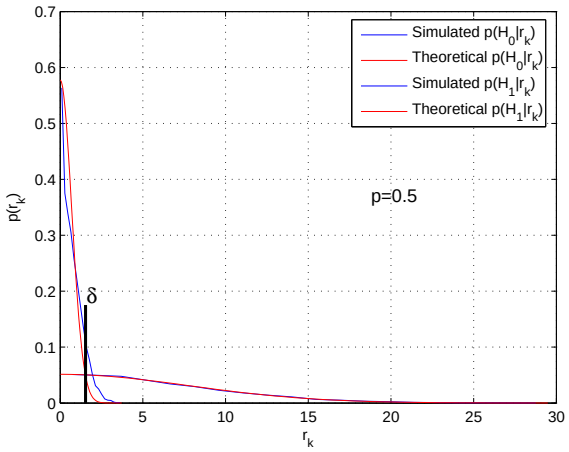

Fig. 3. The theoretical and simulation pdf of $p(H_0|r_k)$ and $p(H_1|r_k)$ with $p = 0.5, \sigma_\gamma = 10V_{RMS}$ and $SNR = 16$ dB for a QPSK constellation.

D. Simulation Results

The performance of the proposed approach has been studied by means of computer simulation for an uncoded QPSK DMT system. All results are obtained by using standard ADSL parameters with in total 256 carriers, $M = 12$ or 24 guard carriers. The simple Bernoulli-Gaussian impulsive noise model $\gamma_k = g_k b_k$ was used, where g_k is the Bernoulli process with probability $P(g_k = 1) = p$, and b_k is zero mean white Gaussian noise. In this study, we fixed $p = 0.001$ and set the standard deviation of b_k to $\sigma_\gamma = 10V_{RMS}$, where V_{RMS} is the average RMS value of the transmitted block symbols.

First, we compare the performance between shift register decoding and least-squares decoding with 256 carriers and $M = 12$ guard carriers. The simulation results are presented in Fig. 4. The performance of shift register decoding is worse than least-squares decoding at low SNR values since it sums up the background noise in the decoding process.

In a second study, we compare the performance of least-squares decoding by changing the number of guard carriers. the simulation results are presented in Fig. 5. It can be seen from the figures that the performance is near the AWGN case at low SNR values. But the performance in case of the smaller

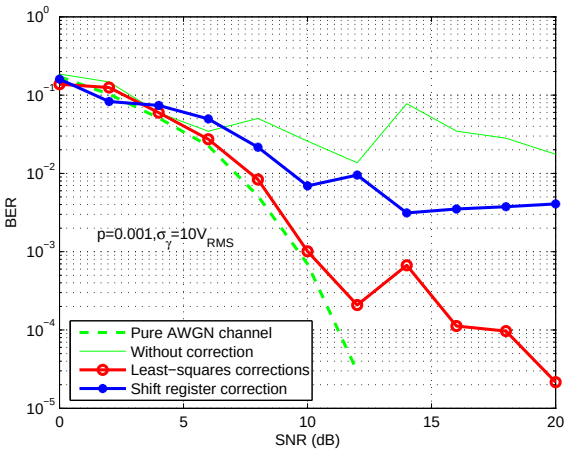

Fig. 4. BER performances of shift register decoding and least-squares decoding for Bernoulli impulses ($\sigma_\gamma = 10V_{RMS}, p = 0.001$) in a QPSK DMT system.

number of guard carriers $m = 12$ converges earlier and offers no further improvement at high SNR values.

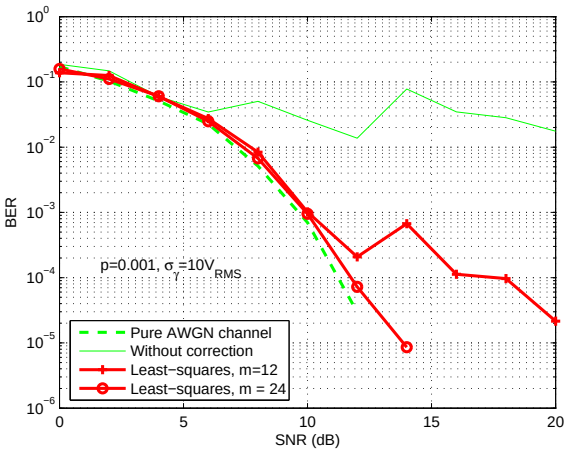

Fig. 5. BER performances of least-squares decoding for Bernoulli impulses ($\sigma_\gamma = 10V_{RMS}, p = 0.001$) in a QPSK DMT system with different numbers of guard carriers.

As the third result, we show performances when increasing the input SNR to 100 dB in order to verify the performance of optimal threshold detection in a wide range of the input SNR. The output SNR is computed instead of the BER to save simulation time. The results are presented in Fig. 6 where dashed lines resulted when assuming the error locations to be known and the solid lines are simulated by using the optimal threshold for detecting the error locations. Parameters are set to $m = 12, \sigma_\gamma = 10V_{RMS}, p = 0.001$. From the figure, we see that the performance curves saturate at higher SNR values when using the optimal threshold detection. This behaviour is expected since false detection of error positions does not depend on the Gaussian background noise any more, but on the signal itself.

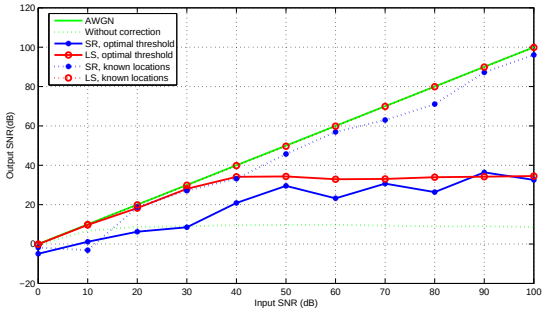

Fig. 6. Performances of the optimal threshold detection for Bernoulli impulses ($\sigma_\gamma = 10V_{RMS}, p = 0.001$) in a QPSK DMT system versus increasing the input SNR.

III. Correction of Clipping Errors

One of the major problems of multicarrier transmission is its high peak-to-average ratio. Different methods have been developed to reduce the peaks at the transmitter side before the non-linearity (limiting A/D converter, amplifier). Nevertheless, if out-of-band power is not of major concern, one may correct the clipping noise at the receiver side using analog codes. Clipping noise can be seen as impulse noise. Figure 7 sketches the clipping of higher amplitudes exceeding a certain clipping amplitude. The clipped signal components shown in the lower diagram indeed show up as impulse noise.

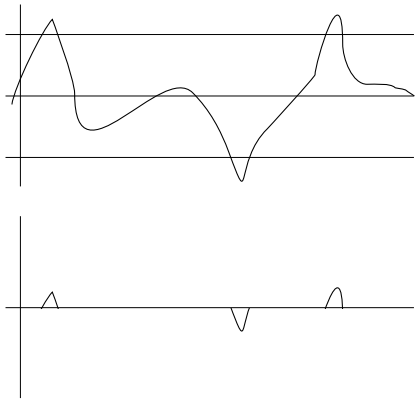

Fig. 7. Impulsive clipping noise
(upper: original signal,
lower: clipped signal components)

The difference to Section II is the position of the impulse noise addition. Here, it is transmitter-sided. One would thus equalize the channel transfer function at the receiver before the clipping correction. The processing chain is then given by

[S/P] $\longrightarrow$ [QAM-Mapping] $\longrightarrow$ [IFFT] $\longrightarrow$ [CP Extension] $\longrightarrow$ [Channel] $\longrightarrow$ [CP Deletion] $\longrightarrow$ [FFT] $\longrightarrow$ [DFT-domain 1-tap equalizer] $\longrightarrow$ [IFFT] $\longrightarrow$ [Erasure Setting] $\longrightarrow$ [Analog Decoding in DFT domain] $\longrightarrow$ [P/S]

Using analog codes for clipping correction has been published earlier by the authors in [2], [3]. We extend this work by applying the least-squares approach in Eqn. (5). We recompute the case with a clipping detection threshold at 98 % of the clipping level without any filtering in place. Figure 8 shows the clipping gain relative to the clipping level normalized to the RMS value. The results cleary outlines the advantages of least-squares computations. although shift register syndrome extension would be more natural since the information is located in DFT domain and would be less complex.

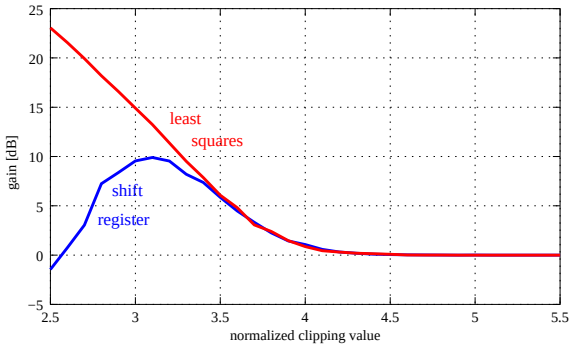

Fig. 8. Clipping correction gain: shift-register versus least squares (Parameters from [2], [3]: DFT length N=64, redundancy $2 \times M = 2 \times 12$)

IV. Conclusions

We studied impulse and clipping noise correction by a least-squares approach following threshold decisions to locate the errors. We pointed out that these impulsive disturbances can drastically be reduced as long as the error positions can be detected. The threshold for impulse/clipping detection has been computed for a simplified impulse-noise model. We also observed that recursive syndrome extension is no suitable alternative correction procedure.

References

[1] F. Abdelkefi , P. Duhamel, F. Albgerge, "Impulsive Noise Cancellation in Multicarrier Transmission," *IEEE Trans. on Comm.*, Vol. 53, No. 1, pp. 94-106, Jan. 2005

[2] W. Henkel, "Peak-to-Average Ratio Reduction with Analog Codes," in proc. *4. OFDM-Fachgespräch and 1st International OFDM-Workshop*, Hamburg, Sept. 21-22, 1999.

[3] W. Henkel, "Analog Codes for Peak-to-Average Ratio Reduction," in proc. *3rd ITG Conf. Source and Channel Coding*, Munich, Germany, Jan. 2000.

[4] Z. Wang and G. B. Giannakis, "Wireless Multicarrier Communications: where Fourier meets Shannon," *IEEE Signal Processing Mag.*, vol. 47, pp. 29-48, May 2000.

[5] Z. Wang and G. B. Giannakis, "Complex-Field Coding for OFDM over Fading Wireless Channels," *IEEE Trans. on Inform. Theory*, vol. 49, no. 3, March 2003.